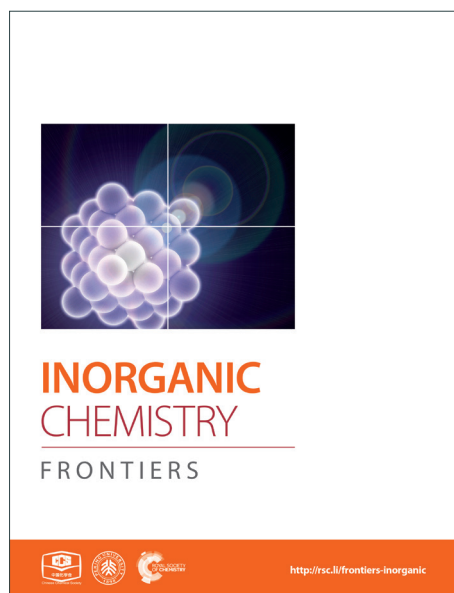
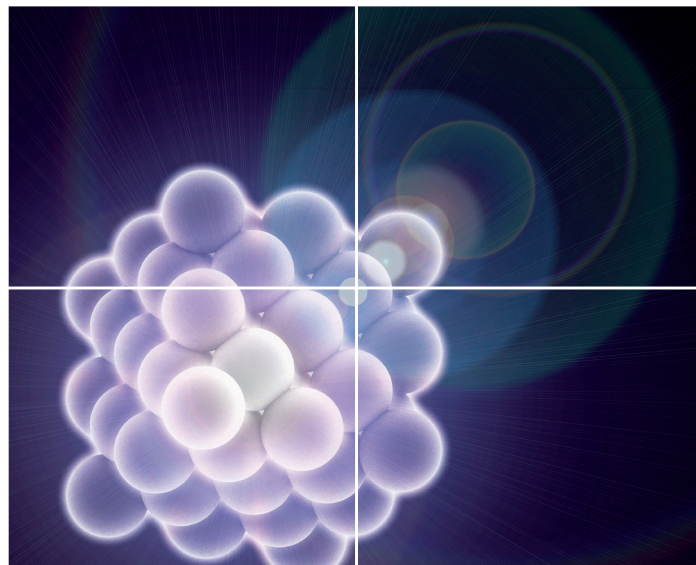


INORGANIC CHEMISTRY

FRONTIERS

Accepted Manuscript



This is an *Accepted Manuscript*, which has been through the Royal Society of Chemistry peer review process and has been accepted for publication.

Accepted Manuscripts are published online shortly after acceptance, before technical editing, formatting and proof reading. Using this free service, authors can make their results available to the community, in citable form, before we publish the edited article. We will replace this *Accepted Manuscript* with the edited and formatted *Advance Article* as soon as it is available.

You can find more information about *Accepted Manuscripts* in the [Information for Authors](#).

Please note that technical editing may introduce minor changes to the text and/or graphics, which may alter content. The journal's standard [Terms & Conditions](#) and the [Ethical guidelines](#) still apply. In no event shall the Royal Society of Chemistry be held responsible for any errors or omissions in this *Accepted Manuscript* or any consequences arising from the use of any information it contains.

Syntheses, X-ray structures, catalytic activity and magnetic properties of two new coordination polymers of Co(II) and Ni(II) based on benzenedicarboxylate and linear N,N'-donor Schiff base linker

Biswajit Bhattacharya[†], Dilip Kumar Maity[†], Pradip Pachfule[§], Enrique Colacio[#] and Debajyoti Ghoshal^{†*}

[†] Department of Chemistry, Jadavpur University, Jadavpur, Kolkata, 700 032, India

[§] Physical/Materials Chemistry Division, CSIR-National Chemical Laboratory, Dr. Homi Bhabha Road, Pune-411008, India

[#] Departamento de Química Inorgánica, Universidad de Granada, 18071-Granada, Spain.

E-mail: dghoshal@chemistry.jdvu.ac.in

Abstract: Two isostructural coordination polymers based on Co(II) and Ni(II), {[M(*azpy*)₃(*p-bdc*)₂(H₂O)₄].(CH₃OH)₂(H₂O)₃]_n [where M = Co (1) and Ni (2); *azpy* = *N,N'*-bis-pyridin-4-ylmethylene-hydrazine and *p-bdc* = 1,4-benzenedicarboxylate], have been synthesized using mixed ligand systems at room temperature and characterized by single-crystal X-ray diffraction and other physicochemical methods. Structure determination reveals that both the complexes crystallize in the monoclinic space group *C2/c* and exhibit one-dimensional (1D) ladder like structures constructed by *p-bdc* and *azpy* ligands in which Schiff base (*azpy*) linkers serve as a bridging as well as pendent ligands. These pendent ligands are involved in H-bonding and π - π interactions with lattice water, methanol molecules and bridging *azpy* ligands, to form the 3D supramolecular structure. Notably, both the frameworks efficiently catalyze the *Knoevenagel* condensation reactions of a wide range of substituted benzaldehydes with active methylene compounds in heterogeneous medium under environmentally friendly conditions and the products were obtained in excellent yields. These catalysts were also found to exhibit excellent recyclability and re-usability without any significant loss of activity. The variable temperature magnetic study of both compounds was carried out and their magnetic properties justified on the basis of their crystal structure.

Introduction

The functional coordination polymer (CP) and/or metal–organic framework (MOF) is nowadays a very popular name in the fields of inorganic and materials research due to its hybrid nature and synthetic tunability.¹ Moreover, this class of molecules has versatile applications like gas storage,² separation,³ proton conductance,⁴ sensing,⁵ drug delivery,⁶ magnetism,⁷ and heterogeneous catalysis.⁸ Out of the above applications of MOFs, heterogeneous catalysis was one of the earliest and efficiently demonstrated applications due to the catalysis-friendly features of MOFs such as poor solubility in common organic solvents, large surface areas and extraordinary porosity, flexibility to afford open channels and ordered pore with catalyst active functionalities.⁹

It has been noticed that several organic transformations along with many condensation reactions such as aldol condensation,¹⁰ aza-Michael condensation,¹¹ Henry reaction,¹² Pechmann reaction,¹³ Friedlander condensation¹⁴ and Knoevenagel condensation¹⁵ *etc.* have been successfully carried out using conventional solid catalysts. Among these reactions, the Knoevenagel condensation of aldehydes with compounds containing activated methylene groups in presence of a weak base has been widely employed in synthetic organic chemistry right from the syntheses of small molecules to the elegant intermediates of anti-hypertensive drugs and calcium antagonists.¹⁶ Different types of solid bases like inorganic salts (Al_2O_3 , ZnCl_2 , $\text{KF-Al}_2\text{O}_3$),¹⁷ zeolite,¹⁸ calcite,¹⁹ basic MCM-41 silica,²⁰ amine-functionalized mesoporous zirconia,²¹ amine-functionalized superparamagnetic nanoparticles²² and chitosan hydrogel²³ *etc.* are nowadays preferred very much as catalysts for the Knoevenagel condensation. The reaction protocol using heterogeneous solid base catalyst, over trivial organic base; is important from an environmental perspective as these can be easily separated by simple filtration. As stated before, the MOFs having all the advantages of heterogeneous catalyst; can act as a nice catalyst if some basic sites could be functionalized in its surroundings.^{8,9} There are established strategies which were adopted to make a MOF based catalyst, for example; inclusion of open metal sites in the nodes, and incorporation of different active functional groups in the organic linkers to improve the catalytic activity of coordination polymers.^{8,9} The inclusion of base functionalized groups (such as, NH_2 , pyridine) in the framework has been well studied for heterogeneous catalysis,^{8,9} but the use of milder Schiff base in such processes is not very common.

Recently, our group has made extensive contribution on the synthesis of mixed ligand MOF with Schiff base functionalized linkers.²⁴ These linkers effectively decorated the pore walls with Schiff base which played a crucial role in selective CO₂ capture behavior of the aforesaid frameworks.²⁴ Moreover, it is worth mentioning that the mixed ligand variety of MOFs have some inherent advantages like flexibility as well as stability in their framework structures. Thus, based on these facts, we were tempted to see if such Schiff base functionalized MOFs can be designed; that might be useful in base-catalyzed reaction, which can reinforced the chemical implication of MOFs along with its all-around physical properties.

Here we have synthesized two isostructural mixed ligand coordination polymers containing pendent Schiff base functionalized ligand with the general formulae $\{[M(azpy)_3(p-bdc)_2(H_2O)_4](CH_3OH)_2(H_2O)_3\}_n$ [where M = Co (**1**) and Ni (**2**); *azpy* = *N,N'*-bis-pyridin-4-ylmethylene-hydrazine and *p-bdc* = 1,4-benzenedicarboxylate]. The single-crystal X-ray structure shows one-dimensional (1D) ladder like structure. Both the compounds are found to achieve significant catalytic activity and reusability towards Knoevenagel condensation as solid base catalyst. To the best of our knowledge, the reported compounds are the most efficient examples of coordination polymers that have been used heterogeneously to catalyze the Knoevenagel condensation reaction till date. The variable temperature magnetic study also corroborates the structure of both the complexes.

Materials

N,N'-bis-pyridin-4-ylmethylene-hydrazine (*azpy*) was synthesized by the procedures reported earlier.²⁵ High purity cobalt(II) nitrate hexahydrate, nickel(II) nitrate hexahydrate, terephthalic acid, substituted benzaldehydes, malononitrile and ethyl cyanoacetate were purchased from the Sigma-Aldrich Chemical Company Inc. and used as received. All other chemicals were of AR grade and were used as received.

Physical measurements

Elemental analyses (carbon, hydrogen, and nitrogen) were performed using a Perkin–Elmer 240C elemental analyzer. Infrared spectra (4000–400 cm⁻¹) were taken on KBr pellet, using Perkin–Elmer Spectrum BX-II IR spectrometer. Thermal analysis (TGA) was carried out on a METTLER TOLEDO TGA 850 thermal analyzer under nitrogen atmosphere (flow rate: 50 cm³ min⁻¹) at the temperature range 30–600 °C with a heating rate of 2 °C/min. X-ray powder

diffraction (PXRD) patterns in different states of the sample were recorded on a Bruker D8 Discover instrument using Cu-K α radiation. All low pressure gas adsorption experiments (up to 1 bar) were performed on a Quantachrome Quadrasorb automatic volumetric instrument. ^1H NMR spectra were recorded at ambient temperature in CDCl_3 with tetramethylsilane as internal standard. The chemical shifts (δ) and coupling constants (J) were expressed in ppm and Hz, respectively on Bruker Avance 300 instrument. Variable temperature (2–300 K) magnetic susceptibility measurements on polycrystalline samples were carried out with a Quantum Design SQUID MPMS XL-5 device operating at different magnetic fields.

Synthesis of $\{[\text{Co}_2(\text{azpy})_3(\text{p-bdc})_2(\text{H}_2\text{O})_4] \cdot (\text{CH}_3\text{OH})_2(\text{H}_2\text{O})_3\}_n$ (1). An aqueous solution (20 mL) of disodium 1,4-benzenedicarboxylate ($\text{Na}_2\text{p-bdc}$) (1 mmol, 0.210 g) was mixed with a methanolic solution (20 mL) of *N, N'*-bis-pyridin-4-ylmethylene-hydrazine (*azpy*) (1 mmol, 0.210 g) and stirred for 20 min to mix it well. $\text{Co}(\text{NO}_3)_2 \cdot 6\text{H}_2\text{O}$ (1 mmol, 0.281 g) was dissolved in 20 ml of water. Then in a crystal tube 4 ml of Co(II) solution was slowly and carefully layered with the 8 ml of abovementioned mixed-ligand solution using a 2 ml of buffer solution (1:1 of water and MeOH) in between the two solution. The tube was sealed and kept undisturbed at room temperature and after one week red colored block shaped single crystals suitable for X-ray diffraction analysis were obtained at the wall of the tube. Crystals were separated and washed with MeOH/water(1:1) mixture and air dried (Yield 79%). Anal. Calc. for $\text{C}_{54}\text{H}_{60}\text{Co}_2\text{N}_{12}\text{O}_{17}$ ($M_r = 1266.99$): C, 51.19; H, 4.77; N, 13.26. Found: C, 51.29; H, 4.92; N, 13.11. IR spectra (in cm^{-1}): $\nu(\text{C}=\text{N})$, 1569; $\nu(\text{C}-\text{O})$, 1310-1230; $\nu(\text{CH}-\text{Ar})$, 3100-2900 and $\nu(\text{C}=\text{C})$, 1600-1440.

Synthesis of $\{[\text{Ni}_2(\text{azpy})_3(\text{p-bdc})_2(\text{H}_2\text{O})_4] \cdot (\text{CH}_3\text{OH})_2(\text{H}_2\text{O})_3\}_n$ (2). This complex has been synthesized by following the same procedure as for **1** using $\text{Ni}(\text{NO}_3)_2 \cdot 6\text{H}_2\text{O}$ (1 mmol, 0.280 g) instead of $\text{Co}(\text{NO}_3)_2 \cdot 6\text{H}_2\text{O}$. Shiny green single crystals suitable for X-ray diffraction analysis were obtained after one month (Yield 64%). Anal. Calc. for $\text{C}_{54}\text{H}_{60}\text{Ni}_2\text{N}_{12}\text{O}_{17}$ ($M_r = 1266.52$): C, 51.21; H, 4.78; N, 13.27. Found: C, 51.35; H, 4.63; N, 13.41. IR spectra (in cm^{-1}): $\nu(\text{C}=\text{N})$, 1568; $\nu(\text{C}-\text{O})$, 1320-1210; $\nu(\text{CH}-\text{Ar})$, 3100-2900 and $\nu(\text{C}=\text{C})$, 1600-1440.

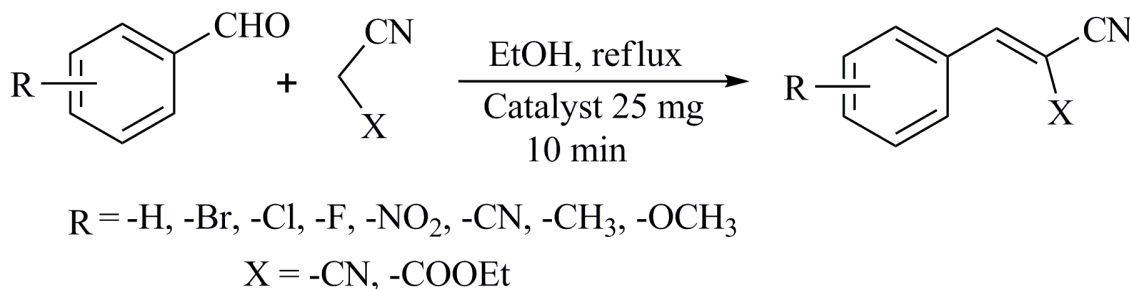
Crystallographic data collection and refinement

Suitable single crystals of **1** and **2** were mounted on the tips of glass fibers with commercially available super glue. X-ray single crystal data collection for both the crystals were performed at room temperature using Bruker APEX II diffractometer, equipped with a normal focus, sealed

tube X-ray source with graphite monochromated Mo-K α radiation ($\lambda = 0.71073 \text{ \AA}$). The data were integrated using SAINT²⁶ program and the absorption corrections were made with SADABS.²⁷ Both the structures were solved by SHELXS 97²⁸ using Patterson method and followed by successive Fourier and difference Fourier synthesis. Full matrix least-squares refinements were performed on F^2 using SHELXL-97²⁸ with anisotropic displacement parameters for all non-hydrogen atoms. In case of **1** and **2**, the occupancy of one lattice water molecule (O4W) was fixed at 0.5 before final refinement. All the hydrogen atoms except the hydrogen of one lattice water (O4W) were fixed geometrically by HFIX command and placed in ideal positions in case of both structures. In **1**, one of the H atoms on O1W are found in two fold disorder and these are fixed considering both 0.5 occupancies from the Fourier map. All calculations were carried out using SHELXL 97, SHELXS 97, PLATON v1.15,²⁹ ORTEP-3v2,³⁰ WinGX system Ver-1.80³¹ and TOPOS.³² Crystallographic and structure refinement data of all compounds are given in Table 1. The selected bond lengths, bond angles are displayed in Table 2 & 3.

General procedure for the Knoevenagel condensation

The Knoevenagel condensations between substituted benzaldehydes and active methylene compounds were carried out according to the following procedure. A mixture of the substituted benzaldehyde (10 mmol), malononitrile or ethyl cyanoacetate (10 mmol) and 25 mg of catalyst (compound **1** or **2**) in ethanol (20 mL) were taken in a round bottom flask and heated to reflux for 10 min (Scheme 1). After completion of the reaction, the catalysts were separated by filtration and washed with ethanol (3 x 10 mL). The combined filtrates were concentrated and the crude reaction products were purified by column chromatography over silica gel (mesh 60–120) using a petroleum ether-ethyl acetate mixture as eluent to give the desired product. The products were then analyzed by ¹H NMR, elemental analysis and compared with authentic samples.



Scheme 1 Knoevenagel condensation reaction catalyzed by compounds **1** and **2**.

Structural description of $\{[M_2(\text{azpy})_3(\text{p-bdc})_2(\text{H}_2\text{O})_4]\cdot(\text{CH}_3\text{OH})_2(\text{H}_2\text{O})_3\}_n$ [M = Co (1) and Ni (2)]. Compounds **1** and **2** are isostructural and both of them crystallize in monoclinic space group $C2/c$. The single crystal structure analysis reveals that both the compounds originate a one-dimensional (1D) ladder structure connected by the 1,4-benzenedicarboxylate (*p-bdc*) and organic linkers (*azpy*). The asymmetric unit of **1** and **2** comprises of one Co(II)/Ni(II) center, one *p-bdc*, one and half *azpy* ligand and two coordinated water molecules. There is one methanol and one and half water molecules present as guest molecules in the lattice. Here, each hexacoordinated metal atom shows a distorted octahedral geometry with the MO_4N_2 core [Fig. 1(a) for **1** and Fig. S1(a) for **2**] which is reflected by their *cisoid* and *transoid* angles along the metal center (Table 2 for **1** and Table 3 for **2**). The coordination around each M(II) is furnished by two carboxylate oxygen atoms (O1 and O4^a where $a = 1/2+x, 1/2+y, z$ for **1** and $a = 1/2+x, 1/2+y, z$ for **2**) of two different bridging 1,4-benzenedicarboxylate, two nitrogen atoms (N1 and N5) of one bridging and one pendent *azpy* ligands and two coordinated water molecules (O1W and O2W) [Fig. 1(a) for **1** and Fig. S1(a) for **2**]. In compound **1**, the Co(II)-O bond lengths are in the range of 2.0546(17)-2.1710(19) Å and Co(II)-N bond length varies from 2.152(2)-2.182(2) Å (Table 2); whereas in case of **2**, the Ni(II)-O and Ni(II)-N bond lengths are 2.0452(17)-2.1203(16) Å and 2.096(2)-2.123(2) Å, respectively (Table 3). Here, each 1,4-benzenedicarboxylate binds in a bridging monodentate fashion and each 1,4-benzenedicarboxylate connects two different M(II) centres to creates a chain with metal to metal separation of 11.395 Å and 11.365 Å in **1** and **2**, respectively. Two such chains are connected by *azpy* to form the 1D ladder like structure [Fig. 1(b) for **1** and Fig. S1(b) for **2**] where the pendent *azpy* ligands are exist like an antenna of the structure in both sides of the ladder.

Topological analysis of the 1D ladder by TOPOS³² software suggests the formation of a 3-connected uninodal net with Schläfli symbol $\{4^2.6\}$ [Fig. 1(c) for **1** and Fig. S1(c) for **2**]. In the crystal packing, these 1D ladders are stitched by H-bonding constructed by the interaction between the coordinated and lattice water molecules. The lattice methanol molecules are also H-bonded with lattice water molecules and nitrogen atom (N4) of pendent *azpy* ligand (Table S1 for **1** and Table S2 for **2**). In addition to that there are intermolecular π - π interactions with in the pyridyl rings of inter-sheet adjacent bridging *azpy* and pendent *azpy* ligands (centroid-centroid distances are in the range of 3.825(2)-3.914(2) Å and 3.8406(14)-3.9006(17) Å for **1** and **2**, respectively) [Table S3 for **1** and Table S4 for **2**]. These cooperative supramolecular interactions

(H-bonds and π - π interactions) convert the ladder structure into a three-dimensional (3D) supramolecular arrangement [Fig. 2(a) for **1** and Fig. S2(a) for **2**]. The potential solvent-accessible void volume, calculated using PLATON,²⁹ suggests 16.80% and 21.10% void volume to the total crystal volume after of **1** and **2**, respectively, after the removal of the guest and coordinated solvent molecules.

Framework stability: thermogravimetric (TG) and powder X-ray diffraction (PXRD) analysis

Thermogravimetric analyses (TGA) and powder X-ray diffraction (PXRD) measurements were carried out to study the stability of the frameworks compounds. TGA of compounds **1** and **2** was performed in the temperature range of 30–500 °C under a nitrogen atmosphere. The TGA profile of compound **1** (Fig. 3) indicates a weight loss of ~9.4% at 100 °C, which corroborates the removal of all guest solvent (three water and two methanol) molecules (cal. 9.3%). The second step was observed at 115 °C with a weight loss of ~15.9%, indicating the removal of coordinated water molecules (cal. 15%). Then the desolvated framework is stable up to 180 °C. After that, it gradually decomposes into unidentified products. Similarly compound **2** (Fig. 3), shows a stepwise release of methanol and water molecules. The first step indicates the release of three lattice water and two lattice methanol molecules (calc. wt loss = 9.32%; exp. wt loss ~ 9.41%) at 115 °C, and the second one corresponds to the release of the other four coordinated water molecules at 130 °C (calcd. wt loss = 15%, total exp. wt loss ~ 15.54%). The desolvated framework of **2** is stable up to 240 °C without any further weight loss.

The PXRD patterns of compounds **1** and **2** are shown in Figs. 4 and 5, respectively. For both the compounds, there are good correspondences of the different peaks in the simulated and as-synthesized patterns are found which indicates the phase purity of the as-synthesized compounds. In cases of desolvated framework, the PXRD patterns are almost similar with the simulated as well as the as-synthesized pattern only with some loss of intensities. This indicates that the heated samples, there is no structural changes in the frameworks even upon removal of the lattice solvent molecule.

Adsorption properties

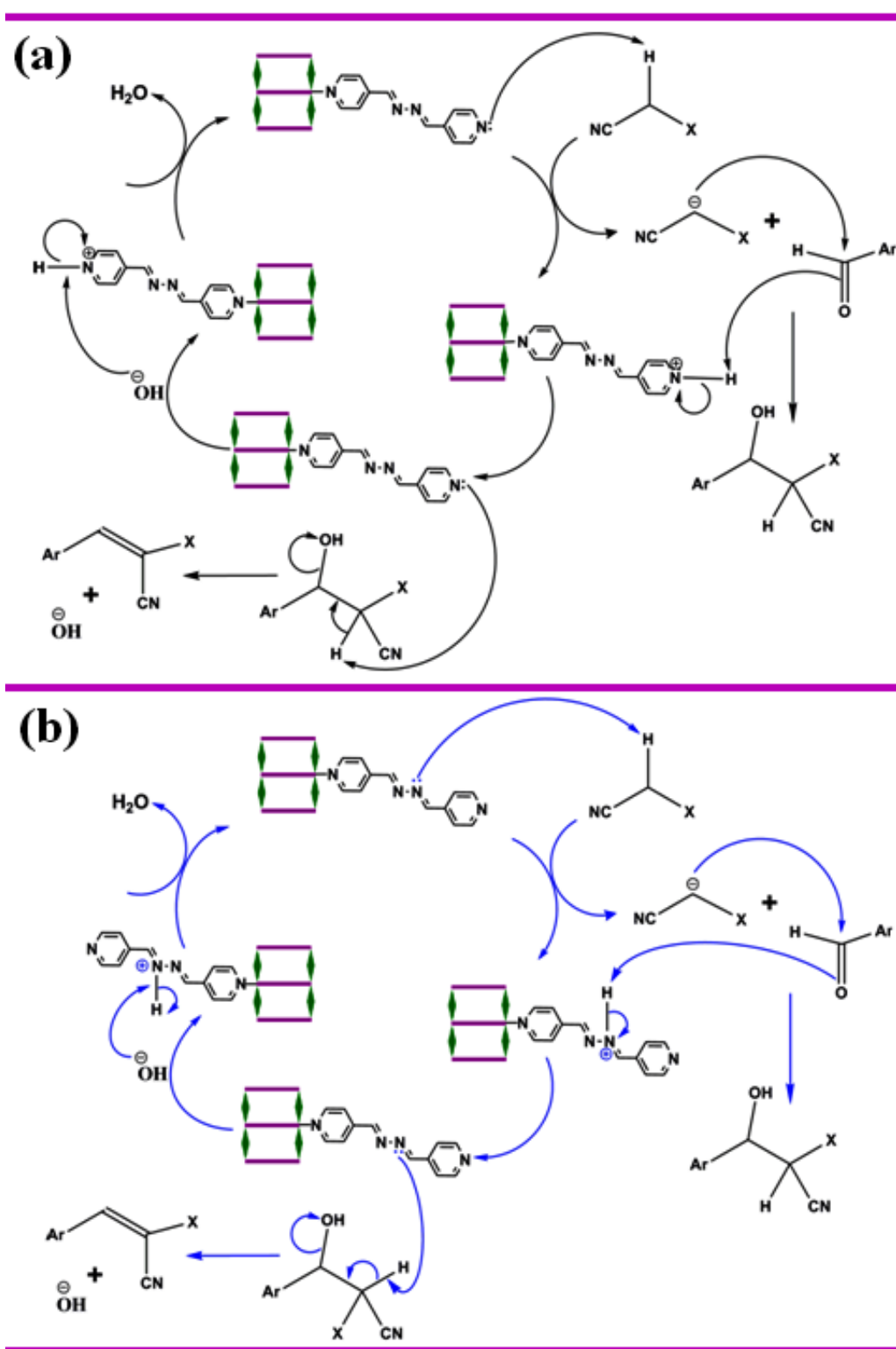
From the structural analysis it is observed that both the structure have measurable voids. Considering their identical structure we took the most stable Ni(II) analogue (**2**) as a representative to study the permanent porosity and the nature thereof. The dehydrated framework

of compound **2** was subjected to sorption studies with N₂ (kinetic diameter 3.64 Å) and CO₂ (kinetic diameter 3.3 Å) at 77 K and 273 K, respectively (Fig. 6a and Fig. 6b). The sample of **2** was prepared by a thorough washing of crystals with CHCl₃ followed by evacuation at 150 °C for 3 h. The N₂ sorption isotherm (Fig. 6a) shows a type II profile, with the final uptake of 29 cc g⁻¹, suggesting only surface adsorption. While for the same compound, CO₂ adsorption isotherm shows the final uptake is 2.78 wt % (14.14 cc g⁻¹) as the pressure approaches to 800 torr and desorption profile does not follow the adsorption curve (Fig. 6b). The sorption profile shows a hysteresis retaining 4 cc g⁻¹ of CO₂ even at very low P/P₀ (0.001). This is probably due to the strong interaction of CO₂ molecules with the pendent pyridyl nitrogen atom and –CH=N– moiety of *azpy* ligand. These interactions may facilitate the selectivity in adsorption as well as the kinetic trapping of gas molecules, retaining of some CO₂ molecules.

Catalytic Knoevenagel condensation reactions

The Knoevenagel reaction is well known and is very important in reaction methodology, not only as a weak base-catalyzed model reaction but also a reaction that generates a C-C bond. To probe the catalytic activity of **1** and **2**, we have chosen Knoevenagel condensation reaction of substituted benzaldehydes with methylene compounds (malononitrile and ethyl cyanoacetate). The results of the catalytic Knoevenagel condensation reaction for different substrates are summarized in Table 4. The yields of the respective adduct of different benzaldehydes with malononitrile and ethyl cyanoacetate clearly indicates an efficient catalytic activity. Both of the compounds do not have effective pore and thus the catalytic reactions mainly occurred onto the surface of **1** and **2**. The Plausible mechanism of MOF (**1** or **2**) catalyzed Knoevenagel condensation of different substituted aromatic aldehydes with active methylene compounds is depicted in Scheme 2. Both the compounds contain –CH=N– groups of bridging/pendent *azpy* ligands and also free pyridyl moieties of pendent *azpy*. These can function as highly reactive base catalyst under such mild conditions. Here the pyridyl/imine nitrogen acts as a Brønsted proton scavenger from the active methylene group of malononitrile or ethyl cyanoacetate, which is acidic in nature due to presence of two strong electron withdrawing groups.³³ The conjugate base generated here is stable due to conjugation with the cyano or acetate groups. Now, this anion makes nucleophilic attack to the carbonyl carbon atom of the substituted aromatic aldehydes.³³ After two cycles of protonation and deprotonation, the MOF catalysts return back to

the original structure and the product is released from the surface of the MOF. The probable mechanism has been depicted in Scheme 2.



Scheme 2 Probable mechanisms of Knoevenagel condensation reaction catalyzed by compounds **1** and **2**. (a) Proton scavenges by pyridyl nitrogen (black arrow) of pendent *azpy* ligand. (b) Proton scavenges by imine nitrogen (blue arrow) of bridging and pendent *azpy* ligand.

The influence of solvent on the Knoevenagel condensation catalyzed by **1** or **2** was investigated using the model reaction between benzaldehyde and malononitrile and the results are shown in Table 5. It is evident that only in CH₃OH and C₂H₅OH, the reactions got completed within 10 min at refluxing condition, with high yields. However, at 50 °C in C₂H₅OH/CH₃OH, the reaction did not complete, as the yield of the reaction is much higher at refluxing condition. Thus it may infer that for a certain time, with the increase of temperature the yield of the condensation reaction increases. For solvents like acetonitrile, benzene, CHCl₃ and THF, which are less polar than ethanol/methanol, the Knoevenagel condensation did not occur at all within 10 min time either at 50 °C or in refluxing condition (Table 5, entries 1–7).

Considering moderate reaction temperature and we took more environment friendly ethanol as the solvent for studying our model Knoevenagel condensation catalyzed by **1** or **2**. At first, a blank reaction of benzaldehyde with malononitrile in refluxing ethanol has performed to confirm that the reaction does not proceed in absence of a MOF catalyst. Then the catalysis has been performed with different substrates. In case of benzaldehyde substituted with electron withdrawing groups (–NO₂, –CN, etc.), the yield increases, whereas the electron donating substituents (–CH₃, –OCH₃, etc.) on the aromatic ring considerably decreases the yield (Table 4). In case of electron withdrawing groups the possibility of attack of the carbanion (generated from the active methylene group) on the carbonyl carbon is much higher compared to that of electron donating groups. Condensation of substituted benzaldehyde with various substrates possessing active methylene groups is shown in Table 4. The substituents with electron withdrawing nature stabilizes the carbanion (via conjugation) compared to those having electron donating nature. So malononitrile displays the maximum conversion compared to the ethyl cyanoacetate. When substituents are present in the ortho position of the aromatic ring the yield of the product has been minimized. This could be attributed to the steric hindrance at the reaction site.

The key advantages of the use of heterogeneous catalysts are easy recovery of the catalyst from the reaction mixtures and its reuse which has been done in all instances in present study. In

order to check the stability of the MOF catalysts, we have also characterized the recovered MOFs. After the catalytic reactions were over, the MOF was recovered by centrifugation, washed thoroughly with ethanol and dried. The recovered MOF catalyst was then subjected to X-ray powder diffraction and IR spectral analysis. Comparison of IR spectra (Fig. 7) and X-ray diffraction patterns (Figs. 4 and 5) of the as-synthesized and the recovered MOF convincingly demonstrated that the structural integrity of the compound remained unaltered after the Knoevenagel condensation reactions. For the recycling study, we performed Knoevenagel condensation reactions using the same model reaction between benzaldehyde and malononitrile with recovered MOFs **1** and **2** in ethanol. After recycling five times and to our surprise; the condensation yield was as high as that of the first cycle (Table 6). With our results, we made a comparative study to see how well our present protocol holds up with respect to existing solid catalysts.³⁴ The results of our findings are summarized in Table 7, shows that the reported protocol offer considerably improvement over existing reports not only in terms of catalyst loading but also in terms of reaction time and yield.

Magnetic properties of **1** and **2**

The $\chi_{\text{M}}T$ value for compound **1** at room temperature ($3.21 \text{ cm}^3 \text{ mol}^{-1} \text{ K}$) is significantly larger than the spin-only value for a high-spin Co(II) ion ($S = 3/2$, $1.875 \text{ cm}^3 \text{ mol}^{-1} \text{ K}$ with $g = 2$), which is indicative of the unquenched orbital contribution of the Co(II) ion in distorted octahedral geometry (Fig. 8). The $\chi_{\text{M}}T$ product remains almost constant from room temperature to 100 K and then slightly decreases reaching a value of $2.11 \text{ cm}^3 \text{ mol}^{-1} \text{ K}$ at 2 K. Because the shortest Co-Co distance through the ligand is 11.395 \AA , the exchange interaction between the Co(II) ions can be considered as negligible. Therefore, this decrease in $\chi_{\text{M}}T$ is most likely due to spin-orbit coupling (SOC) effects rather than intra- and intermolecular antiferromagnetic interactions. The magnetic susceptibility data for **1** were analyzed by introducing SOC effects through the Hamiltonian: $\hat{H} = \alpha\lambda\hat{L} \cdot \hat{S} + \Delta[\hat{L}_z^2 - \hat{L}(\hat{L} + 1)/3] + \beta H \cdot (-\alpha\hat{L} + g_e\hat{S})$ where λ is the spin-orbit coupling parameter, α is the orbital reduction factor, and Δ the axial and orbital splitting of the T_1 term (Fig. 8). Using the MAGSAKI package,³⁵ the best-fit was found with the values $\lambda = -126 \text{ cm}^{-1}$, $\alpha = 1.395$, $\Delta = -691 \text{ cm}^{-1}$ and $\text{TIP} = 428 \times 10^{-6} \text{ cm}^3 \text{ mol}^{-1}$, with an agreement factor $R = 2.9 \times 10^{-5}$. The negative value of Δ agrees well with the tetragonally compressed octahedral geometry of the CoO_4N_2 coordination environment in **1**.

The temperature dependence of the $\chi_{\text{M}}T$ product for compound **2** ($\chi_{\text{M}}T$ being the molar magnetic susceptibility per Ni(II) ion) is displayed in Fig. 9. The $\chi_{\text{M}}T$ value at room temperature of $1.26 \text{ cm}^3 \text{ K mol}^{-1}$ is typical for non-interacting Ni(II) ions ($S = 1$) with $g > 2$, as expected for the long Ni-Ni distances through the ligand (15.64 \AA) and the space (12.03 \AA). When temperature is lowered, the $\chi_{\text{M}}T$ keeps almost constant until 15 K and then sharply decreases to a value of $0.61 \text{ cm}^3 \text{ K mol}^{-1}$ at 2 K. The decrease at low temperature is due to the zero-field splitting of the $^4\text{A}_{2\text{g}}$ ground state in O_h geometry, due to a combination of the tetragonal distortion and spin-orbit coupling. We have further analyzed the magnetic properties of **2** by using the Hamiltonian $\mathbf{H} = D[\mathbf{S}_z^2 - S(S + 1)/3] + g\mu_B\mathbf{H}\mathbf{S}$, where S is the spin ground state and D is the axial anisotropy, μ_B is the Bohr magneton and H the applied magnetic field. Simultaneous fitting of the magnetization and magnetic susceptibility data to the above Hamiltonian using the program *PHI*³⁶ afforded the following magnetic parameters: $|D| = 5.2 \text{ cm}^{-1}$, $g = 2.15$ and $\text{TIP} = 340 \times 10^{-6} \text{ cm}^3 \text{ mol}^{-1}$. The D_{Ni} value is in agreement with those reported in the literature.³⁷

Conclusions

In summary, we have successfully synthesized two mixed ligand one-dimensional (1D) ladder like coordination polymers of Co(II) and Ni(II) containing pendent linear Schiff base linkers. Both the coordination polymers contain an imine group as well as a non-coordinated pyridyl groups which have been efficiently conducts the Knoevenagel condensation of different substituted benzaldehydes with different methylene active compounds, as solid basic catalyst. During the catalytic reaction they display excellent conversions in a short reaction time and to carry out this reaction there is no need for inert atmosphere, as the MOF based catalysts are highly stable in air. It is interesting to note here, that among all the tested solvents, more economic and environmental friendly ethanol gives significantly good yield. Moreover, at the end of the each catalytic reaction, the catalysts were easily separated from the reaction system by filtration and then conveniently recycled and reused several times without any loss of activity. The attractive features of these types of coordination polymer catalysts could help to reduce disposal costs and could prove themselves to be significant to the chemical industry for their use in greener and continuous chemical processes. Therefore, the compounds **1** and **2** are the nice recyclable catalytic systems which can function reliably in ethanol medium producing promising

yield for base catalyzed Knoevenagel condensation. Further investigation of designing more coordination polymer based catalyst and also investigation of other base catalyzed reactions using coordination polymers are currently in progress.

Acknowledgements

Authors gratefully acknowledge the financial assistance given by CSIR, Govt. of India (Grant to DG). BB and DKM acknowledges UGC for the research fellowship. The X-ray diffractometer facility under the DST-FIST program of Department of Chemistry (JU) is also gratefully acknowledged. We gratefully acknowledge Dr. Rahul Banerjee at NCL, Pune, India, for the gas adsorption study and some valuable discussion during the preparation of the manuscript.

Electronic supplementary information (ESI) available:

Tables of H-bonding and π - π interaction interactions, structural figure of compounds reported in this paper and ^1H NMR of all known products found in the reactions related to catalysis, elemental analysis study of the isolated products are available as ESI. The structure reported in this paper having the CCDC reference numbers 981262 and 981263. For ESI and crystallographic data in CIF or other electronic format see DOI:

References

- (a) O. M. Yaghi, M. O'Keeffe, N. W. Ockwig, H. K. Chae, M. Eddaoudi and J. Kim, *Nature*, 2003, **423**, 705; (b) C. Janiak, *Dalton Trans.*, 2003, 2781; (c) S. Kitagawa, R. Kitaura and S.-I. Noro, *Angew. Chem., Int. Ed.*, 2004, **43**, 2334; (d) G. Férey, C. Mellot-Draznieks, C. Serre, F. Millange, J. Dutour, S. Surblé and I. Margiolaki, *Science*, 2005, **309**, 2040; (e) A. K. Cheetham, C. N. R. Rao and R. K. Feller, *Chem. Commun.*, 2006, 4780; (f) K. Biradha, A. Ramanan and J. J. Vittal, *Cryst. Growth Des.*, 2009, **9**, 2969; (g) A. U. Czaja, N. Trukhanb and U. Müller, *Chem. Soc. Rev.*, 2009, **38**, 1284; (h) N. R. Champness, *Dalton Trans.*, 2011, **40**, 10311.
- (a) R. Vaidhyanathan, S. S. Iremonger, K. W. Dawson and G. K. H. Shimizu, *Chem. Commun.*, 2009, 5230; (b) O. K. Farha, A. Ö. Yazaydın, I. Eryazici, C. D. Malliakas, B. G. Hauser, M. G. Kanatzidis, S. T. Nguyen, R. Q. Snurr and Joseph T. Hupp, *Nature Chem.*, 2010, **2**, 944; (c) K. Jayaramulu, S. K. Reddy, A. Hazra, S. Balasubramanian and T. K. Maji, *Inorg. Chem.*, 2012, **51**, 7103; (d) K. Sumida, D. Stück, L. Mino, J.-D. Chai, E. D. Bloch, O. Zavorotynska, L. J. Murray, M. Dincă, S. Chavan, S. Bordiga, M. H.-Gordon and J. R. Long, *J. Am. Chem. Soc.*, 2013, 135, 1083.

- 3 (a) X. Zhao, B. Xiao, J. A. Fletcher, K. M. Thomas, D. Bradshaw and M. J. Rosseinsky, *Science*, 2004, **306**, 1012; (b) H. K. Chae, D. Y. Siberio-Perez, J. Kim, Y. Go, M. Eddaoudi, A. J. Matzger, M. O'Keeffe and O. M. Yaghi, *Nature*, 2004, **427**, 523; (c) W. Lu, D. Yuan, D. Zhao, C. I. Schilling, O. Plietzsch, T. Muller, S. Bräse, J. Guenther, J. Blümel, R. Krishna, Z. Li and H.-C. Zhou, *Chem. Mater.*, 2010, **22**, 5964; (d) P. Pachfule and R. Banerjee, *Cryst. Growth Des.*, 2011, **11**, 5176; (e) G. Férey, C. Serre, T. Devic, G. Maurin, H. Jobic, P. L. Llewellyn, G. D. Weireld, A. Vimont, M. Daturif and J.-S. Changg, *Chem. Soc. Rev.*, 2011, **40**, 550.
- 4 (a) S. Sen, N. N. Nair, T. Yamada, H. Kitagawa and P. K. Bharadwaj, *J. Am. Chem. Soc.*, 2012, **134**, 19432; (b) S. Horike, D. Umeyama and S. Kitagawa, *Acc. Chem. Res.*, 2013, **46**, 2376; (c) X.-Y. Dong, R. Wang, J.-B. Li, S.-Q. Zang, H.-W. Houa and T. C. W. Makac, *Chem. Commun.*, 2013, **49**, 10590; (d) T. Panda, T. Kundu and R. Banerjee, *Chem. Commun.*, 2013, **49**, 6197; (e) T. Yamada, K. Otsubo, R. Makiurac and H. Kitagawa, *Chem. Soc. Rev.*, 2013, **42**, 6655.
- 5 (a) G. J. Halder, C. J. Kepert, B. Moubaraki, K. S. Murray and J. D. Cashion, *Science*, 2002, **298**, 1762; (b) Y. Bai, G. J. He, Y. G. Zhao, C. Y. Duan, D. B. Dang and Q. J. Meng, *Chem. Commun.*, 2006, 1530; (c) B. Gole, A. K. Bar and P. S. Mukherjee, *Chem. Commun.*, 2011, **47**, 12137; (d) S. S. Nagarkar, B. Joarder, A. K. Chaudhari, S. Mukherjee and S. K. Ghosh, *Angew. Chem. Int., Ed.*, 2013, **52**, 2881.
- 6 (a) P. Horcajada, C. Serre, M. Vallet-Regi, M. Sebban, F. Taulelle, G. Férey, *Angew. Chem., Int. Ed.*, 2006, **45**, 5974; (b) K. E. deKrafft, Z. G. Xie, G. H. Cao, S. Tran, L. Q. Ma, O. Z. Zhou and W. B. Lin, *Angew. Chem., Int. Ed.*, 2009, **48**, 9901; (c) I. Imaz, M. Rubio-Martinez, L. Garcia-Fernandez, F. Garcia, D. Ruiz-Molina, J. Hernando, V. Puentes, D. MasPOCH, *Chem. Commun.*, 2010, **46**, 4737.
- 7 (a) P. Kanoo, C. Madhu, G. Mostafa, T. K. Maji, A. Sundaresan, S. K. Pati and C. N. R. Rao, *Dalton Trans.*, 2009, 5062; (b) M. Kurmoo, *Chem. Soc. Rev.*, 2009, **38**, 1353; (c) P. Mahata, S. Natarajan, P. Panissod and M. Drillon, *J. Am. Chem. Soc.*, 2009, **131**, 10140; (d) Z. M. Wang, K. L. Hu, S. Gao and H. Kobayashi, *Adv. Mater.*, 2010, **22**, 1526; (f) Tripuramallu, B. K.; Manna, P.; Reddy, S. N.; Das, S. K. *Cryst. Growth Des.* **2012**, *12*, 777; (e) S. Goswami, A. Adhikary, H. S. Jena, S. Biswas and S. Konar, *Inorg. Chem.*, 2013, **52**, 12064.
- 8 (a) T. Uemura, R. Kitaura, Y. Ohta, M. Nagaoka and S. Kitagawa, *Angew. Chem., Int. Ed.*, 2006, **45**, 4112; (b) J. Lee, O. K. Farha, J. Roberts, K. A. Scheidt, S. T. Nguyen and Joseph T. Hupp, *Chem. Soc. Rev.*, 2009, **38**, 1450; (c) M. C. Das, S. Xiang, Z. Zhang and B. Chen, *Angew.*

Chem., Int. Ed., 2011, **50**, 10510; (d) R. Sen, D. Saha and S. Koner, *Chem.Eur. J.* 2012, **18**, 5979; (e) B. Gole, A. K. Bar, A. Mallick, R. Banerjee and P. S. Mukherjee, *Chem. Commun.*, 2013, **49**, 7439.

9 (a) J. S. Seo, D. Whang, H. Lee, S. I. Jun, J. Oh, Y. J. Jeon and K. Kim, *Nature*, 2000, **404**, 982; (b) S. Hasegawa, S. Horike, R. Matsuda, S. Furukawa, K. Mochizuki, Y. Kinoshita and S. Kitagawa, *J. Am. Chem. Soc.*, 2007, **129**, 2607; (c) J. Gascon, U. Aktay, M. D. Hernandez-Alonso, G. P. M. van Klink, F. Kapteijn, *J. Catal.*, 2009, **261**, 75; (d) S. Neogi, M. K. Sharma and P. K. Bharadwaj, *J. Mol. Catal. A: Chem.*, 2009, **299**, 1; (e) M. Savonnet, S. Aguado, U. Ravon, D. Bazer-Bachi, V. Lecocq, N. Bats, C. Pinel and D. Farrusseng, *Green Chem.*, 2009, **11**, 1729; (f) T. Uemura, N. Yanaia and S. Kitagawa, *Chem. Soc. Rev.*, 2009, **38**, 1228; (c) L. Ma, C. Abney and W. Lin, *Chem. Soc. Rev.*, 2009, **38**, 1248; (g) A. Dhakshinamoorthy, M. Opanasenko, J. Čejka and H. Garcia, *Adv. Synth. Catal.*, 2013, **355**, 247.

10 (a) M. L. Kantam, B. M. Choudary, Ch. V. Reddy, K. K. Rao and F. Figueras, *Chem. Commun.*, 1998, 1033; (b) S. Abelló, F. Medina, D. Tichit, J. P.-Ramírez, Y. Cesteros, P. Salagre and J. E. Sueiras, *Chem. Commun.*, 2005, 1453; (c) A. M. Frey, S. K. Karmee, K. P. de Jong, J. H. Bitter, U. Hanefeld, *ChemCatChem*, 2013, **5**, 594.

11 (a) B. Das and N. Chowdhury, *J. Mol. Catal. A: Chem.*, 2007, **263**, 212; (b) M. Mokhtar, T. S. Saleh, S. N. Basahel, *J. Mol. Catal. A: Chem.*, 2012, **353**, 122.

12 (a) R. Ballini, G. Bosica, D. Livi, A. Palmieri, R. Maggib and G. Sartorib, *Tetrahedron Lett.*, 2003, **44**, 2271; (b) T. Arai, M. Watanabe, A. Fujiwara, N. Yokoyama and A. Yanagisawa, *Angew. Chem., Int. Ed.*, 2006, **45**, 5978.

13 (a) M. Maheswara, V. Siddaiah, G. L. V. Damu, Y. K. Rao, C. V. Rao, *J. Mol. Catal. A: Chem.*, 2006, **255**, 49; (b) P. Kalita and R. Kumar, *Microporous Mesoporous Mater.*, 2012, **149**, 1.

14 (a) J. S. Yadav, P. P. Rao, D. Sreenu, R. S. Rao, V. N. Kumar, K. Nagaiah and A. R. Prasad, *Tetrahedron Lett.*, 2005, **46**, 7249; (b) Z. N. Siddiqui and K. Khan, *New J. Chem.*, 2013, **37**, 1595.

15 (a) N. Kan-nari, S. Okamura, S.-i. Fujita, J.-i. Ozaki and M. Arai, *Adv. Synth. Catal.*, 2010, **9**, 1476; (b) G. B. B. Varadwaj, S. Rana and K. M. Parida, *Dalton Trans.*, 2013, **42**, 5122.

16 (a) E. Knoevenengel, *Chem. Ber.*, 1898, **31**, 2585; (b) G. Jones, *Org. React.*, 1967, **15**, 204;

- (c) L. F. Tietze and P. Saling, *Synlett*, 1992, 281; (d) I. Kim, S. G. Kim, J. Choi and G. H. Lee, *Tetrahedron*, 2008, 64, 664.
- 17 (a) P. S. Rao and R. V. Venkataratnam, *Tetrahedron Lett.*, 1991, 32, 5821; (b) F. Texier-Boullet and A. Foucaud, *Tetrahedron Lett.*, 1982, 23, 4927; (c) G. Dai, D. Shi, L. Zhou and Y. Huaxue, *Chin. J. Appl. Chem.*, 1995, 12, 104.
- 18 T. I. Reddy and R. S. Varma, *Tetrahedron Lett.*, 1997, 38, 1721.
- 19 S. Wada and H. Suzuki, *Tetrahedron Lett.*, 2003, 44, 399.
- 20 (a) K. M. Parida and D. Rath, *J. Mol. Catal. A: Chem.*, 2009, **310**, 93; (b) F. Shang, J. Sun, S. Wua, Y. Yang, Q. Kan and J. Guan, *Microporous Mesoporous Mater.*, 2010, **134**, 44.
- 21 K. M. Parida, S. Mallick, P. C. Sahoo and S. K. Rana, *Appl. Catal., A*, 2010, **381**, 226.
- 22 N. T. S. Phan and C. W. Jones, *J. Mol. Catal. A: Chem.*, 2006, **253**, 123.
- 23 K. R. Reddy, K. Rajgopal, C. U. Maheswari and M. L. Kantam, *New J. Chem.*, 2006, **30**, 1549.
- 24 (a) R. Dey, R. Haldar, T. K. Maji and D. Ghoshal, *Cryst. Growth Des.*, 2011, **11**, 3905; (b) B. Bhattacharya, R. Dey, P. Pachfule, R. Banerjee and D. Ghoshal, *Cryst. Growth Des.*, 2013, **13**, 731; (c) B. Bhattacharya, R. Dey, D. K. Maity and D. Ghoshal, *CrystEngComm*, 2013, **15**, 9457; (d) B. Bhattacharya, R. Haldar, R. Dey, T. K. Maji and D. Ghoshal, *Dalton Trans.*, 2014, **43**, 2272; (e) R. Dey, B. Bhattacharya, P. Pachfule, R. Banerjee and D. Ghoshal, *CrystEngComm*, 2013, DOI: 10.1039/C3CE42028K.
- 25 A. R. Kennedy, K. G. Brown, D. Graham, J. B. Kirkhouse, M. Kittner, C. Major, C. J. McHugh, P. Murdoch and W. E. Smith, *New J. Chem.*, 2005, **29**, 826.
- 26 *SMART (V 5.628)*, *SAINT (V 6.45a)*, *XPREP*, *SHELXTL*, Bruker AXS Inc., Madison, WI, 2004.
- 27 G. M. Sheldrick, *SADABS (Version 2.03)*, University of Göttingen, Germany, 2002.
- 28 G. M. Sheldrick, *SHELXS-97*, *Acta Crystallogr.*, 2008, **A64**, 112.
- 29 A. L. Spek, *Acta Crystallogr.*, 2009, **D65**, 148.
- 30 L. J. Farrugia, *J. Appl. Crystallogr.*, 1997, **30**, 565.
- 31 L. J. Farrugia, WinGX, *J. Appl. Crystallogr.*, 1999, **32**, 837.
- 32 (a) V. A. Blatov, A. P. Shevchenko and V. N. J. Serezhkin, *Appl. Crystallogr.*, 2000, **33**, 1193. (b) V. A. Blatov, L. Carlucci, G. Ciani and D. M. Proserpio, *CrystEngComm*, 2004, **6**, 378.

- 33 (a) R. W. Hein, M. D. Astle and J. R. Shelton, *J. Org. Chem.*, 1961, **26**, 4874; (b) G. Li, J. Xiao and W. Zhang, *Green Chem.*, 2011, **13**, 1828; (c) J. Mondal, A. Modak and A. Bhaumik, *J. Mol. Catal. A: Chem.*, 2011, 335, 236.
- 34 (a) M. Opanasenko, A. Dhakshinamoorthy, M. Shamzhy, P. Nachtigall, M. Horáček, H. Garcia and J. Čejka, *Catal. Sci. Technol.*, 2013, **3**, 500; (b) M. Hartmann and M. Fischer, *Microporous Mesoporous Mater.*, 2012, **164**, 38; (c) S. Ernst, M. Hartmann, S. Sauerbeck and T. Bongers, *Appl. Catal. A*, 2000, **200**, 117; (d) P. Kasinathan, Y.-K. Seo, K.-E. Shim, Y. Kyu Hwang, U.-H. Lee, D. W. Hwang, D.-Y. Hong, S. B. Halligudi and J.-S. Chang, *Bull. Korean Chem. Soc.*, 2011, **32**, 2073.
- 35 H. Sakiyama, *J. Chem. Software*, 2001, **7**, 171.
- 36 N. F. Chilton, R. P. Anderson, L. D. Turner, A. Soncini, K. S. Murray, *J. Comput. Chem.*, 2013, **34**, 1164.
- 37 (a) S. K. Dey, M. S. El Fallah, J. Ribas, T. Matsushita, V. Gramlich and S. Mitra, *Inorg. Chim. Acta*, 2004, **357**, 1517; (b) K. K. Nanda, R. Das, L. K. Thompson, K. Venkatsubramanian and K. Nag, *Inorg. Chem.*, 1994, **33**, 5934; (c) R. Das, K. K. Nanda, K. Venkatsubramanian, P. Paul and K. Nag, *J. Chem. Soc. Dalton. Trans.*, 1992, 1253; (d) P. Mukherjee, M. G. B. Drew, C. J. Gómez-García and A. Ghosh, *Inorg. Chem.*, 2009, **48**, 5848; (e) Z. Q. Pan, K. Ding, H. Zhou, Q. R. Cheng, Y. I. Cheng and Q. M. Huang, *Polyhedron*, 2011, **30**, 2268.

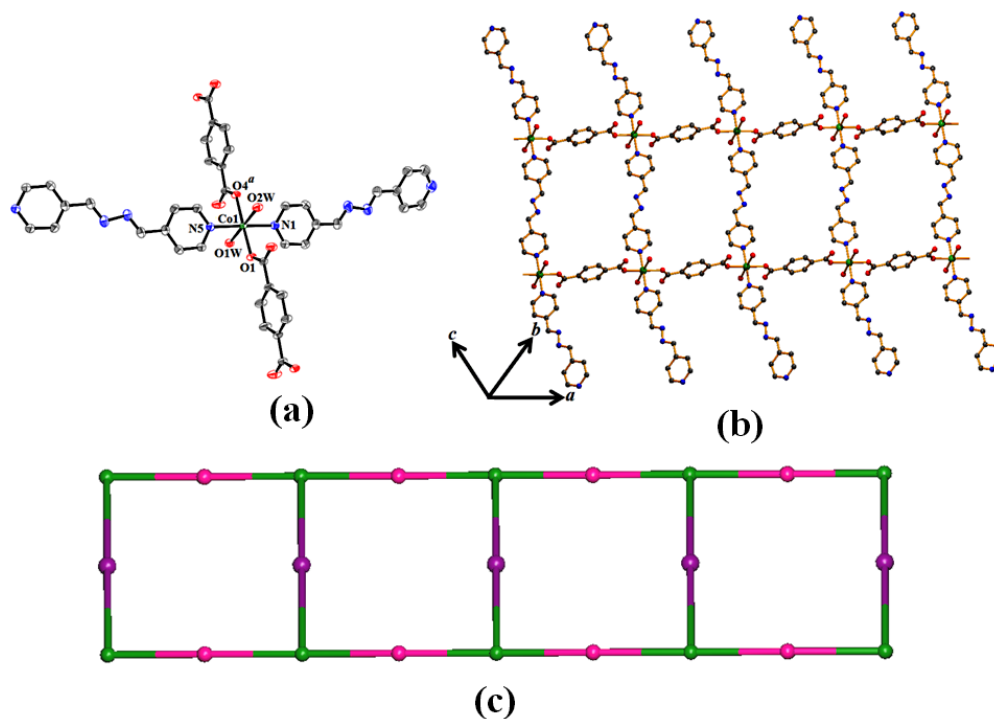
Figures

Fig. 1 (a) ORTEP drawing (40% probability ellipsoid) of **1** showing atom labeling scheme. (b) View of extended 1D ladder structure of compound **1** constructed by 1,4-benzenedicarboxylate, *azpy* ligand and Co(II). (c) Simplified topological representation of 1D ladder in **2**.

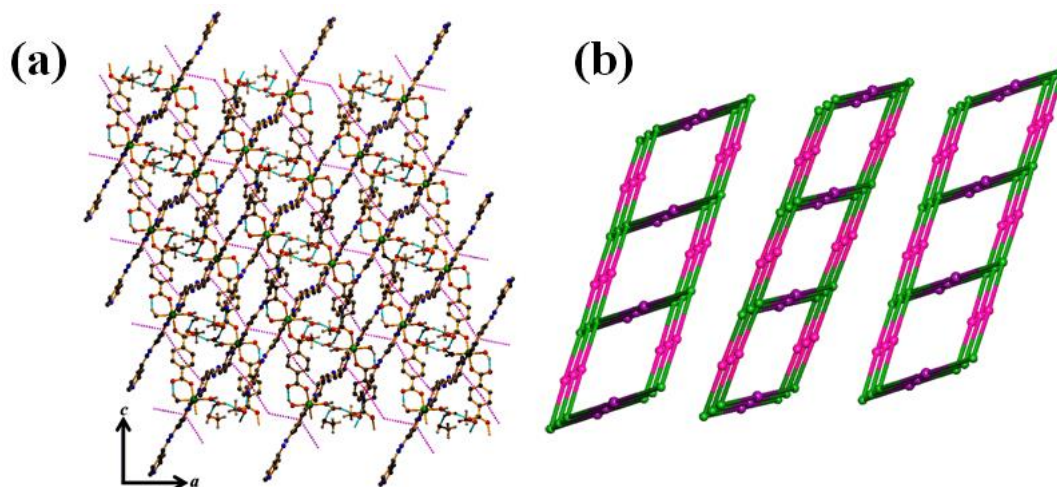


Fig. 2 (a) Supramolecular 3D network in **1** (π - π interaction: pink dotted lines & H-bonding: cyan dotted lines). (b) Simplified topological disposition view of adjacent ladders in **1**.

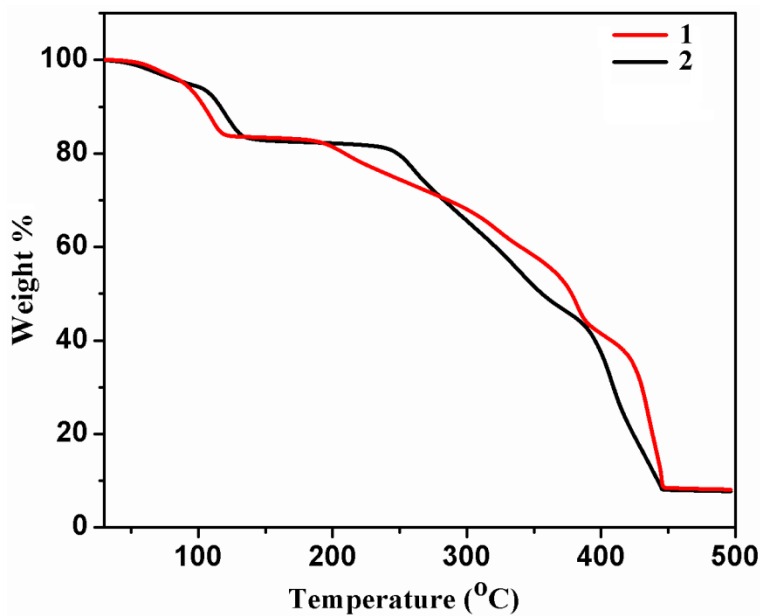


Fig. 3 TGA curves of compounds **1** and **2** in the temperature range 30–500 °C under a nitrogen atmosphere (heating rate 2 °C min⁻¹).

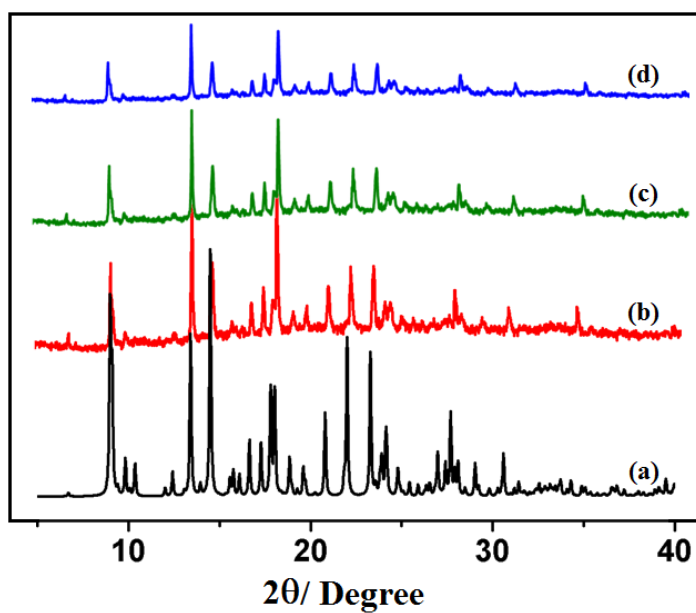


Fig. 4 PXRD patterns in different states: (a) Simulated from X-ray single crystal data; (b) bulk as-synthesized compound; (c) at 150 °C; (d) recovered compound after catalysis of **1**.

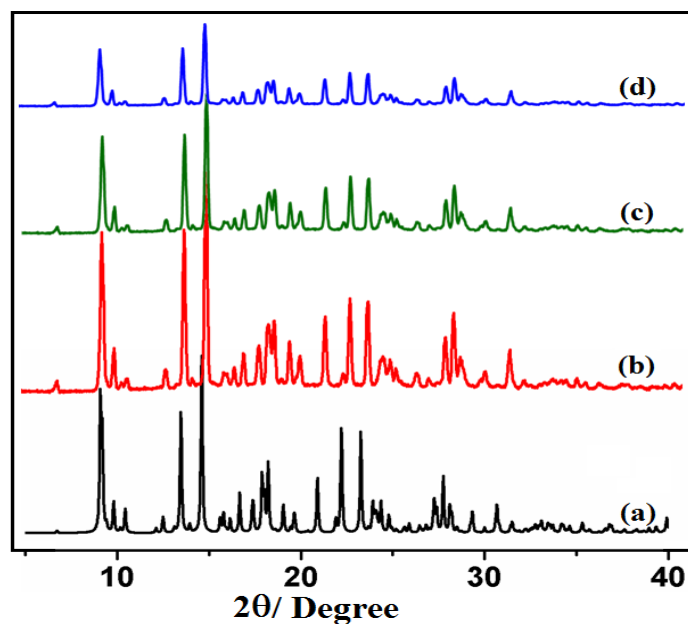


Fig. 5 PXRD patterns in different states: (a) Simulated from X-ray single crystal data; (b) bulk as-synthesized compound; (c) at 150 °C; (d) recovered compound after catalysis of **2**.

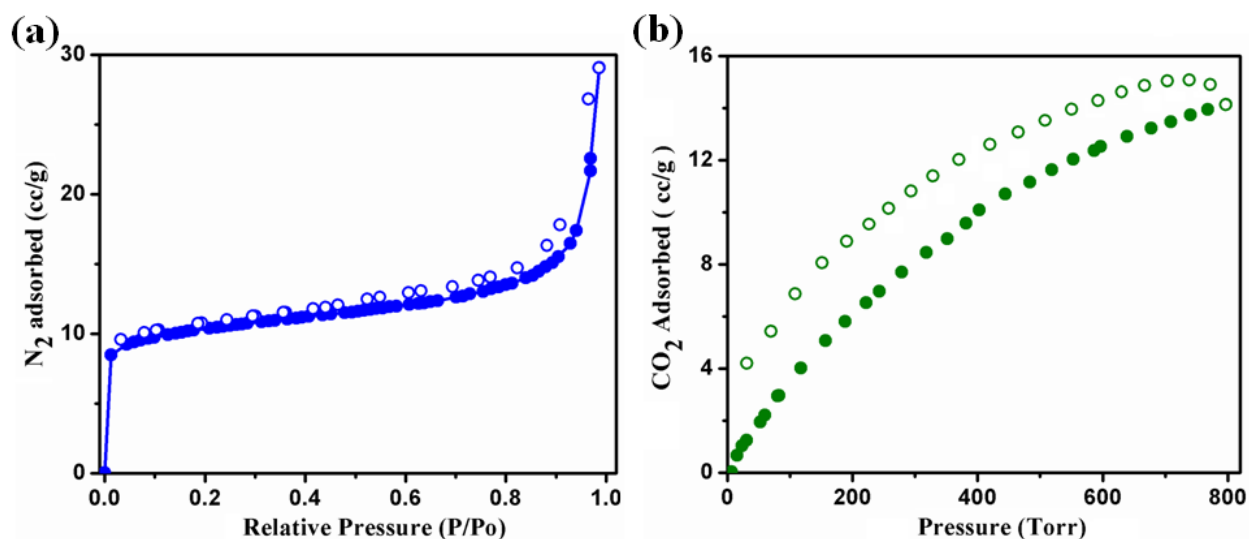


Fig. 6 (a) N₂ adsorption isotherms below 1.0 bar pressure of **2** at 77 K. (b) CO₂ adsorption isotherms below 800 Torr pressure of **2** at 273 K temperature. Filled and open circles represent adsorption and desorption respectively.

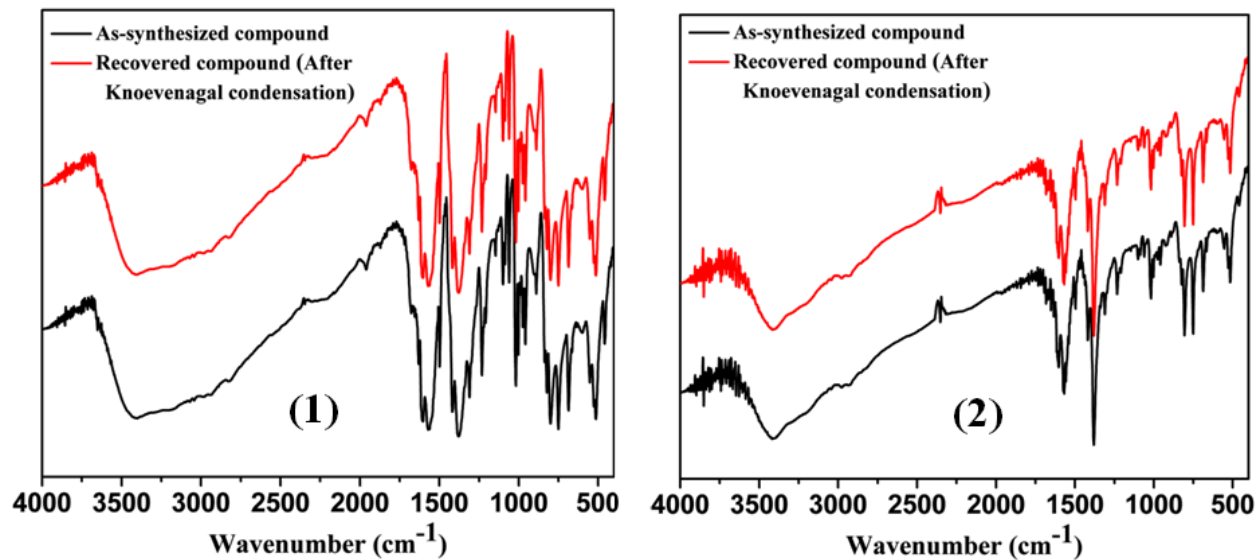


Fig. 7 Comparison of IR spectra of pure and recovered compound after Knoevenagel condensation reaction of **1** and **2**, respectively.

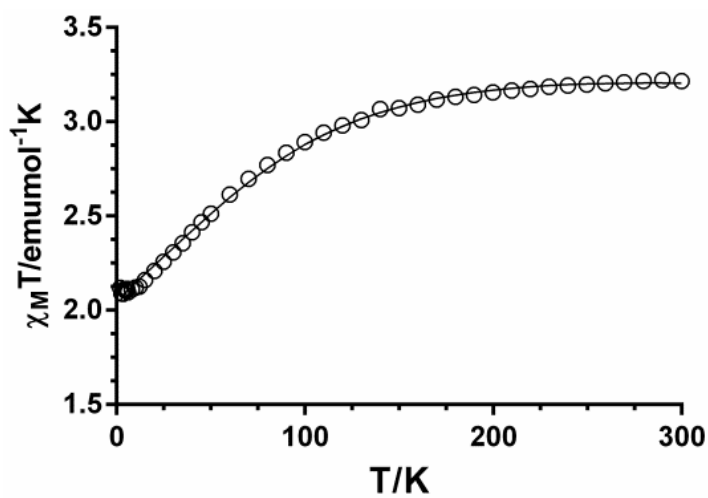


Fig. 8 Temperature dependence of $\chi_M T$ for **1**.

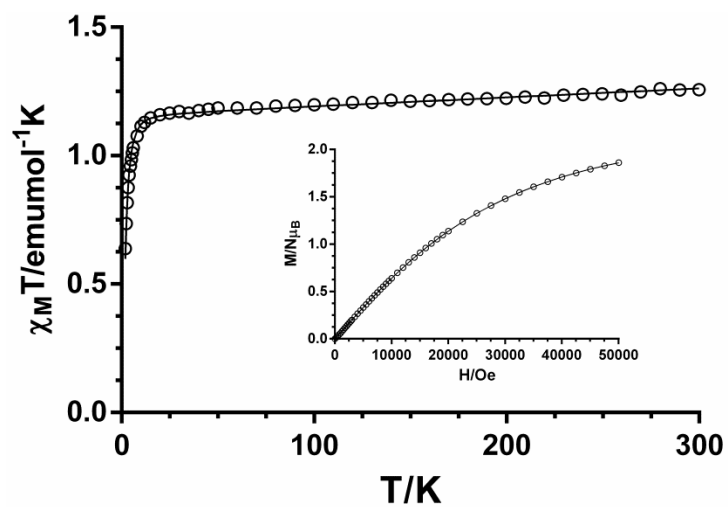


Fig. 9 Temperature dependence of $\chi_M T$ and field-dependence of magnetization at 2 K (inset) for **2**.

Tables:**Table 1** Crystallographic and structural refinement parameters for **1** and **2**

	1	2
Formula	C ₅₄ H ₆₀ Co ₂ N ₁₂ O ₁₇	C ₅₄ H ₆₀ Ni ₂ N ₁₂ O ₁₇
Formula Weight	1266.99	1266.52
Crystal System	Monoclinic	Monoclinic
Space group	<i>C2/c</i>	<i>C2/c</i>
<i>a</i> /Å	19.652(5)	19.6754(3)
<i>b</i> /Å	11.540(5)	11.3812(3)
<i>c</i> /Å	27.611(5)	27.5363(5)
α /°	90	90
β /°	107.031(5)	107.342(1)
γ /°	90	90
<i>V</i> /Å ³	5987(3)	5885.9(2)
<i>Z</i>	4	4
<i>D_c</i> /g cm ⁻³	1.403	1.427
μ /mm ⁻¹	0.632	0.719
<i>F</i> (000)	2624	2632
θ range/°	1.5-27.5	1.5-27.6
Reflections collected	47915	47291
Unique reflections	6852	6795
Reflections <i>I</i> > 2 σ (<i>I</i>)	6057	5990
<i>R</i> _{int}	0.023	0.027
goodness-of-fit (<i>F</i> ²)	1.05	1.12
<i>R</i> 1 (<i>I</i> > 2 σ (<i>I</i>)) ^[a]	0.0386	0.0418
<i>wR</i> 2(<i>I</i> > 2 σ (<i>I</i>)) ^[a]	0.1367	0.1280
$\Delta\rho$ max/min/e Å ³	-0.62, 1.05	-0.51, 0.71

$$^a R_1 = \sum | |F_o| - |F_c| | / \sum |F_o|, wR_2 = [\sum (w(F_o^2 - F_c^2))^2 / \sum w(F_o^2)^2]^{1/2}$$

Table 2 Selected bond lengths (Å) and bond angles (°) for **1**

Co1-O1	2.0546(17)	Co1-O1W	2.1467(19)
Co1-O2W	2.1710(19)	Co1-N1	2.152(2)
Co1-N5	2.182(2)	Co1-O4 ^a	2.0682(17)
O1-Co1-O1W	89.90(6)	O1-Co1-O2W	91.26(6)
O1-Co1-N1	88.46(7)	O1-Co1-N5	90.91(7)
O1-Co1-O4 ^a	176.64(6)	O1W-Co1-O2W	178.20(6)
O1W-Co1-N1	91.09(7)	O1W-Co1-N5	87.77(7)
O1W-Co1-O4 ^a	93.46(6)	O2W-Co1-N1	87.57(7)
O2W-Co1-N5	93.59(7)	O2W-Co1-O4 ^a	85.39(6)
N1-Co1-N5	178.69(7)	O4 ^a -Co1-N1	91.63(7)
O4 ^a -Co1-N5	89.08(7)		

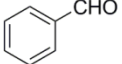
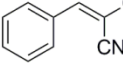
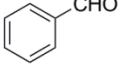
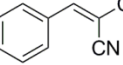
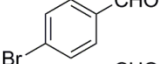
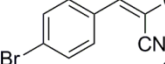
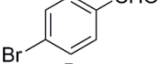
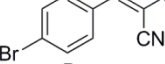
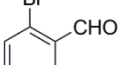
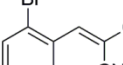
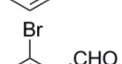
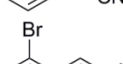
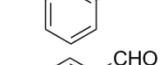
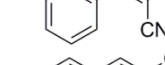
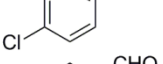
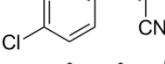
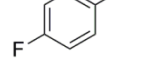
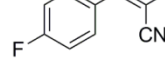
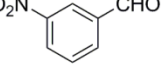
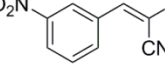
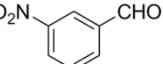
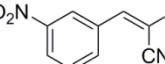
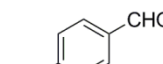
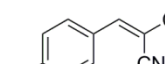
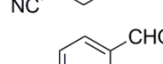
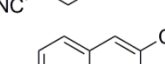
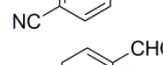
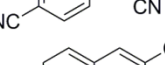
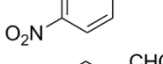
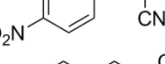
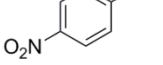
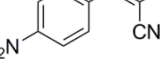
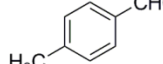
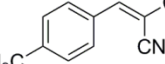
Symmetry code: *a* = 1/2+x, 1/2+y, z.

Table 3 Selected bond lengths (Å) and bond angles (°) for **2**

Ni1-O1	2.0452(17)	Ni1-O1W	2.1051(16)
Ni1-O2W	2.1203(16)	Ni1-N1	2.096(2)
Ni1-N5	2.123(2)	Ni1-O4 ^a	2.0518(17)
O1-Ni1-O1W	88.51(7)	O1-Ni1-O2W	92.17(7)
O1-Ni1-N1	88.57(7)	O1-Ni1-N5	90.78(7)
O1-Ni1-O4 ^a	177.72(6)	O1W-Ni1-O2W	179.31(7)
O1W-Ni1-N1	91.55(7)	O1W-Ni1-N5	87.42(7)
O1W-Ni1-O4 ^a	93.74(7)	O2W-Ni1-N1	88.32(7)
O2W-Ni1-N5	92.72(7)	O2W-Ni1-O4 ^a	85.58(7)
N1-Ni1-N5	178.79(8)	O4 ^a -Ni1-N1	91.03(7)
O4 ^a -Ni1-N5	89.66(7)		

Symmetry code: $a = 1/2+x, 1/2+y, z$.

Table 4 Knoevenagel condensation of various aromatic aldehydes with active methylene compounds catalyzed by compounds **1** and **2**^a

Entry	Aldehyde	X	Product	Time (min)	Isolated Yield (Wt%)	
					Compound 1	Compound 2
1		CN		10	96, 94 ^b	95, 92 ^b
2		COOEt		60	92	92
3		CN		10	93	93
4		COOEt		60	91	91
5		CN		10	92	93
6		COOEt		60	92	92
7		CN		10	95	96
8		CN		10	96	97
9		CN		10	94	94
10		COOEt		60	91	89
11		CN		10	97	97
12		COOEt		60	93	94
13		CN		10	98	97
14		COOEt		10	95	94
15		CN		10	85	83
16		CN		10	82	84
17		COOEt		60	79	81

^aAll reactions were performed with 10 mmol of substrates in 10 ml of absolute ethanol at 80°C using 25 mg of of the as-synthesized compounds **1** or **2**. ^b The fifth run.

Table 5 The influence of solvent on Knoevenagel condensation of benzaldehyde and malononitrile^a

Entry	Solvent	Temp. (°C)	Time (min)	Yield ^b (%)	
				Compound 1	Compound 2
1	C ₆ H ₆	50/80	10	nr	nr
2	CHCl ₃	50/65	10	nr	nr
3	THF	50/65	10	nr	nr
4	CH ₃ CN	50/80	10	nr	nr
5	CH ₃ OH	50	10	82	83
6	CH ₃ OH	65	10	94	93
7	C ₂ H ₅ OH	50	10	54	54
8	C ₂ H ₅ OH	60	10	72	70
9	C ₂ H ₅ OH	70	10	83	86
10	C ₂ H ₅ OH	80	10	96	96

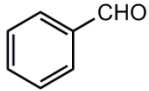
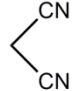
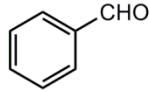
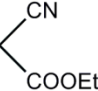
^aReaction condition: Benzaldehyde (10 mmol), malononitrile (10 mmol), compound 1 or 2 (25 mg) in each solvent (10 ml). ^b isolated yield by column chromatography.

Table 6 Reusability of the coordination polymer catalysts 1 and 2

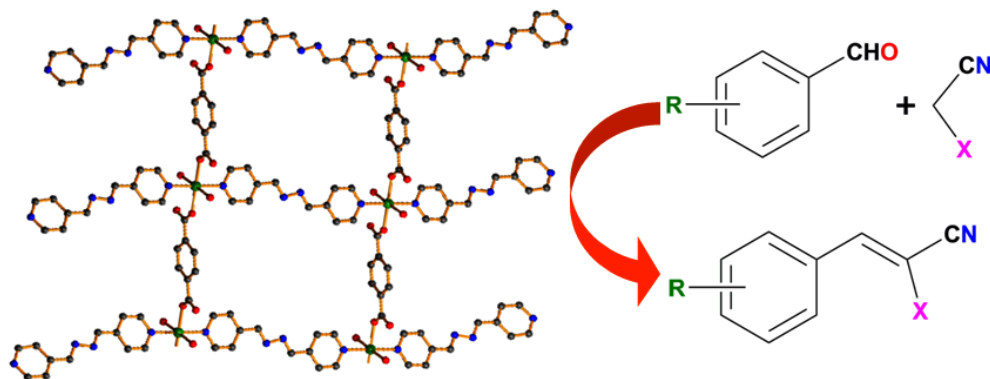
Entry	Recycling runs	Time (min)	Yield ^b (%)	
			Compound 1	Compound 2
1	First	10	96	95
2	Second	10	96	95
3	Third	10	95	94
4	Forth	10	95	93
5	Fifth	10	94	92

^aReaction condition: Benzaldehyde (10 mmol), malononitrile (10 mmol), compound 1 or 2 (25 mg) in each solvent (10 ml). ^b isolated yield by column chromatography.

Table 7 List of catalytic activities of some of the MOFs and common solid catalysts in Knoevenagel condensation of benzaldehyde with malononitrile and ethyl cyanoacetate

Aldehyde	Active methylene compound	Name of Catalyst	Catalys Use (mg)	T/ (°C)	Time	Yield (%)	Reference
		BEA	200	130	4 h	100	34 (a)
		MFI	200	130	6 h	96	34 (a)
		CuBTC	200	130	1 h	100	34 (a)
		Al-MIL-101-NH ₂	30	80	30 min	61	34 (b)
		Fe-MIL-101-NH ₂	30	80	30 min	78	34 (b)
		AIPNO(Amorphous)	200	80	30 min	33	34 (c)
		{[Co(azpy) ₃ (p-bdc) ₂ (H ₂ O) ₄].(CH ₃ OH) ₂ (H ₂ O) ₃ } _n	25	80	10 min	96	This Work
		{[Ni(azpy) ₃ (p-bdc) ₂ (H ₂ O) ₄].(CH ₃ OH) ₂ (H ₂ O) ₃ } _n	25	80	10 min	94	This Work
		BEA	200	130	24 h	66	34 (a)
		MFI	200	130	24 h	39	34 (a)
		CuBTC	200	130	24 h	67	34 (a)
		ED-MIL-101-NH ₂	30	60	15 h	89	34 (d)
		BD-MIL-101-NH ₂	30	60	15 h	98	34 (d)
		DD-MIL-101-NH ₂	30	60	15 h	82	34 (d)
		{[Co(azpy) ₃ (p-bdc) ₂ (H ₂ O) ₄].(CH ₃ OH) ₂ (H ₂ O) ₃ } _n	25	80	1 h	92	This Work
		{[Ni(azpy) ₃ (p-bdc) ₂ (H ₂ O) ₄].(CH ₃ OH) ₂ (H ₂ O) ₃ } _n	25	80	1 h	92	This Work

For Table of Content use



Two isostructural mixed ligand coordination polymers having pendent Schiff base functionalized ligand give excellent catalytic activity on Knoevenagel condensation reactions.